

OPEN-LOOP SUBSPACE IDENTIFICATION OF A FLEXIBLE UNMANNED AERIAL SYSTEM

Raphaela Carvalho Machado¹, David Fernando Castillo Zúniga², Alain de Souza³, Thiago Rosado⁴ & Luiz Carlos Sandoval Góes⁴

¹Universidade Estadual Paulista Júlio de Mesquita Filho (UNESP) - Câmpus de Guaratinguetá, Guaratinguetá, SP, Brasil

²Universidade Estadual Paulista Júlio de Mesquita Filho (UNESP) - Câmpus Experimental de São João da Boa Vista, São João da Boa Vista, SP, Brasil

³Instituto Superior Técnico de Lisboa (IST/ULISBOA), Lisboa, Portugal

⁴Instituto Tecnológico de Aeronáutica (ITA), São José dos Campos, SP, Brasil

Abstract

This paper presents the identification of an Unmanned Aerial System (UAS) with flexible wings from open-loop data using subspace methods. For aerodynamic and flight control systems, a reliable model is important to comprehend the system behaviour and to design a feedback loop, that can be applied as well to minimize the effects of structural flexibility. So, a parametric model identification for flexible aircraft applying subspace techniques was performed. Preliminary results presented in this paper are related to identification using synthetic data. Finally, it is shown the experimental results from the first flight test performed in open-loop operation. The experimental results reveals that subspace methods estimate a state-space model suitable, with better fit for the range of frequencies of the experimental data. Therefore, it was not possible to obtain a representative model for a broader frequency range, however, this is not a limitation of the method, but a persistent excitation problem associated with the limited frequencies in the input signal.

Keywords: flexible aircraft, open-loop subspace identification, flight vehicle system identification, subspace identification method

1. Introduction

In recent years, the demand for unmanned flight has increased, and it has been applied to many serious professional works including: area mapping, agriculture, monitoring, power line inspection, surveying, among others. One advantage of using Unmanned Aerial System (UAS) is that it offers many facilities associated with physical characteristics and easy access when compared to the same activities performed only by humans. For example, the UAS platform named Horus FT-100 is a fixed-wing designed and equipped to attend the *Instituto Militar de Engenharia* (IME), in Brazil, and the Army Technology Center of the Brazilian Army [1].

The demand for unmanned aircraft remotely piloted have instigated research on how to improve aerodynamic efficiency and decrease the aircraft structures' weight. In 2013, the researchers at NASA's Armstrong Flight Research Center, in Edwards, California, designed the PRANDTL-D Sub-Scale Glider, in which the new wing shape significantly increases the aircraft efficiency [23]. In the same year, NASA researchers conducted the first flight of the X-56A Multi-Utility Technology Tested (MUTT), a low-cost, modular and remotely piloted aerial vehicle, designed to explore the behavior of lightweight composite structures.

Due to the continuous growth of the UAS market, with so many applications, it seems justifiable that the Aeronautical Systems Laboratory (LSA) at *Instituto Tecnológico de Aeronáutica* (ITA) became very interested to carry out research on this topic [4, 5, 24–30]. In order to accomplish such goal, researches at ITA have investigated flight vehicle system identification applying different techniques to obtain a representative model for both rigid and flexible aircraft.

In [14], a methodology for system identification based on Linear Parameter Varying (LPV) system is presented. The author used synthetic data from the Xavante AT-26 aircraft to validate the identification methodology proposed. On the other hand, [18] and [10] presented the system identification using experimental data of a fixed-wing unmanned aerial vehicle, called Vector-P. Both longitudinal and lateral-directional motions are identified using the Output-Error Method (OEM) and the results seem to generate a representative model.

Currently, another research group from Laboratory of New Concepts in Aeronautics (LNCA) at ITA is developing research work on the X-HALE-BR (High Altitude Long Endurance) prototype, which had its first flight in 2017. The platform was built at ITA for purposes of flight test, flight stability study and flight control system design, all inserted in the research project Advanced Studies in Flight Physics, funded by *Financiadora de Estudos e Projetos* (FINEP) and *Embraer S.A.*

In [2] is presented the Stability Augmentation System (SAS) designed to be applied further on X-HALE-BR prototype. The closed-loop simulations demonstrated the effectiveness of the SAS feedback. In the same way, [17] applies the Loop-Separation Concept (LSC) to X-HALE, which is the first platform designed and manufactured by the University of Michigan. The main contribution of this work is a new methodology to control Very Flexible Aircraft (VFA) and the preliminary simulated results proved to be an efficient approach. The X-HALE model was implemented in the University of Michigan's Nonlinear Aeroelastic Toolbox (UM/NAST) and used to validate the applied control techniques.

Considering the existing designs of fixed-wing aircraft, such as the mentioned Vector-P and the Telemaster [9], and more specifically, the ones with flexible wings, like the X-HALE-BR aircraft, developed by ITA, and taking advantage of the gap to investigate phenomena associated with structural wing flexibility, this paper deals with an unmanned flexible aircraft, named EOLO. The aircraft started being manufactured in 2015, by Flight Technologies and ACS Aviation Solutions, and had its first flight on 22 August 2019. The objective is to expand the research work on aerodynamic, modeling and system identification at ITA and, mainly, to apply subspace techniques in aeronautic problems.

This paper is organized as follows. Section 2 describes a subspace algorithm applied to both closed-loop and open-loop operation. Section 3 presents the experimental results. Subsection 3.1 gives the EOLO aircraft characteristics. Some experiment trial results for open-loop system identification are presented in subsection 3.2 and, finally, some remarks on the system identification follow in section 4.

2. Subspace Identification Method

The subspace techniques refer to a black-box identification approach applied to identify a model from experimental output-input data. Subspace Identification Method (SIM) have increasing interest over the last two decades, due to their simplicity, numerical robustness and straightforward application to Multiple-Input-Multiple-Output (MIMO) systems. An advantage is that these methods use computational tools, such as QR decomposition and Singular Value Decomposition (SVD), and the identification problem may be solved as an Ordinary Least-Squares (OLS) regression [12].

SIM algorithms are attractive because the state-space form is convenient for estimation, filtering, prediction and control system design. Furthermore, they do not suffer from inconveniences encountered when conventional techniques are applied, as the Prediction Error Method (PEM) and the Output Error Method (OEM). In these cases, it is necessary to solve an optimization problem, where the initial conditions should be given, to provide a parametric model.

Among many subspace algorithms, [11] presents a method denoted SSARX (Space-State AutoRegressive eXogenous models) which uses an Autoregressive exogenous model (ARX), but in a completely different way. The SSARX algorithm applies the estimated Markov parameters obtained from the ARX model to solve the identification problem. According to the results obtained, the algorithm performance seems to be superior to SSNEW (State-Space NEW) algorithm.

The development of another subspace identification method, denoted DSR (Combined Deterministic and Stochastic System Identification and Realization), for both closed and open-loop have been performed in [8]. An advantage is that the innovation estimation is obtained straightforwardly from the input-output data and then, another deterministic identification problem is solved.

In [7], a new algorithm named DSR_e was developed and shown to be as efficient as PEM (Prediction Error Method). [6] also showed that the DSR_e algorithm outperforms the SSNEW, SSARX and PBSID

(Predictor-Based Subspace Identification) methods for closed-loop subspace identification. Therefore, the DSR_e algorithm was chosen to be applied in the system identification of flexible aircraft.

2.1 DSR_e Algorithm

The DSR_e algorithm, proposed by [7] and described in more details in [6], is a direct approach because uses only input-output data to perform the system identification. A special property of this algorithm is that the innovation covariance matrix can be determined directly from a projection of the input-output data matrices, without recursive equations.

In this paper, the DSR_e algorithm proposed by [7], will be called *original* DSR_e , in order to differentiate it from the DSR_e algorithm described in this section, which uses N4SID (Numerical algorithms for Subspace State Space System Identification) tools to solve a deterministic problem after removing the noise from the future data.

The DSR_e algorithm was implemented in Matlab[®] and described in [15], which this algorithm were compared to *original* DSR_e . The results show that both algorithms present similar performance. Figure 1 refers to a flowchart of the computational procedure performed by the algorithm. As can be observed, SVD and QR decomposition are the main tools employed, which are also used in many subspace algorithms.

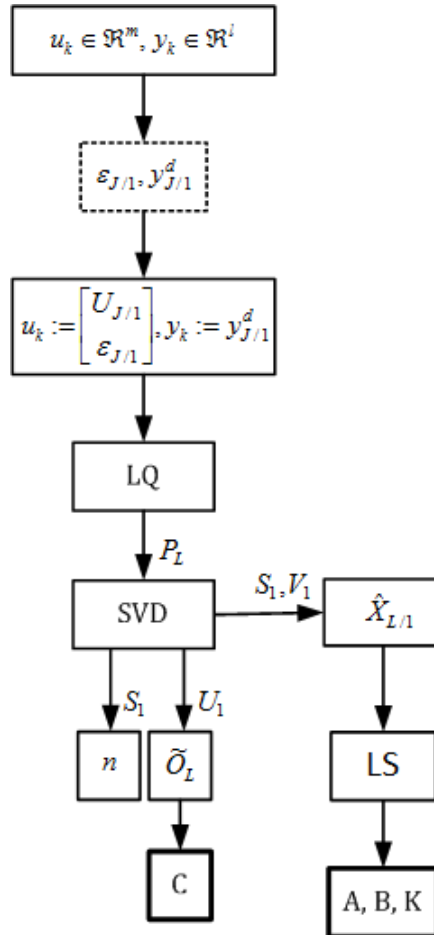


Figure 1 – DSR_e algorithm flowchart.

The algorithm above, just like the original DSR_e , is performed in two main steps. In the first step, the output data are split into a signal part $\mathbf{y}_{J/1}^d$ and an innovation part ε as Equation 1,

$$\mathbf{y}_{J/1} = \mathbf{y}_{J/1}^d + \varepsilon_{J/1} \quad (1)$$

and the second step consists in solving a deterministic identification problem, as addressed in [13].

Applying a SVD decomposition in the projection matrix \mathbf{P}_L , the smallest nonzero singular value of the \mathbf{S}_1 matrix determines the numerical rank of this matrix. These singular values correspond to the model order estimated by the subspace algorithms.

After removing the effect of noise on input data, the system matrices are calculated by solving a deterministic identification problem with the null \mathbf{D} matrix, formulated from Equation 2.

$$\begin{aligned} \mathbf{x}_{k+1} &= \mathbf{A}\mathbf{x}_k + [\mathbf{B} \ \mathbf{K}] \begin{bmatrix} \mathbf{u}_k \\ \boldsymbol{\varepsilon}_k \end{bmatrix} \\ \mathbf{y}_k^d &= \mathbf{C}\mathbf{x}_k \end{aligned} \quad (2)$$

In this step, the new input and output data are defined as follows:

$$\begin{aligned} \mathbf{u}_k : &= \begin{bmatrix} \mathbf{U}_{J/1} \\ \boldsymbol{\varepsilon}_{J/1} \end{bmatrix} \\ \mathbf{y}_k : &= \mathbf{y}_{J/1}^d \end{aligned} \quad (3)$$

where $k = J, J+1, J+2, \dots, N-1$ and $N := N-J$ is the sample number.

3. Discussions on Experiment Trial Results

The first flight test campaign was performed at the *Clube de Modelismo Urbanova* (CMU), in *São José dos Campos-SP* and had the objective of understanding the UAS capabilities and limitations, and also collecting flight data for system identification.

A ground control station, provided by FT *Sistemas*, was employed to remotely control the EOLO aircraft. In general, the facilities are mainly provided by a NI myRIO data acquisition system, linked to a radio communication in high speed used to control the aircraft by a joystick. Many variables were measured and recorded during the flight test programs. As this UAS does not have a landing gear, it was necessary to develop an aircraft launch vehicle.

This section is divided as follows. Subsection 3.1 provides a brief description of the UAS and subsection 3.2 focuses on the open-loop system identification applied to the aircraft longitudinal dynamics.

3.1 EOLO Description

The EOLO aircraft shown in Figure 2, weighs 8.87 kg, has a wing span of 4 m, and a planform area of 0.8460 m², resulting in an aspect ratio of $AR = 18.91$. The Selig S2091 profile, which describes an airfoil with high lift, was applied to manufacture the EOLO wings. Preliminary aerodynamic coefficients were calculated, based on this aerodynamic profile, by [26]. These estimated parameters were used in this paper to provide the aircraft model simulation presented in subsection 3.2.

As modern aircraft designers focus on increasing aerodynamic efficiency and low structural weight, it is increasing the number of aircraft designs with high aspect ratios, combined with the lightweight composite structure. Therefore, this paper analyses an UAS designed with flexible wings just to evaluate the influence of aeroelastic modes during its flight.

The UAS has three control-surfaces deflections, an aileron, a rudder and an elevator. The propulsion system acts along the vehicle's fuselage, only in X-axis. Therefore, the propulsive thrust is a force that does not generate moment. The aircraft mechanical parameters, including the geometry, mass and mass moments of inertia used for simulation, are summarized in Table 1.

Table 1 – Mechanical characteristics of the EOLO aircraft.

Reference geometry	Total mass	Inertia
$S=0.846 \text{ m}^2$	$m=8.87 \text{ kg}$	$I_{xx}=2.53 \text{ kg.m}^2$
$\bar{c}=0.2311 \text{ m}$		$I_{yy}=1.60 \text{ kg.m}^2$
$b=4 \text{ m}$		$I_{zz}=3.96 \text{ kg.m}^2$

Accurate values of the mass moments of inertial were obtained from the Mass Properties Lab at the Institute of Aeronautics and Space (IAE) in 2019, using a Space Electronics device, model KSR 1320.



Figure 2 – EOLO aircraft.

The measurement principle applied for estimation of the mass moment of inertia is based on the inverted torsion pendulum concept.

In [26] is obtained an estimate of rigid aerodynamics coefficients using the Athena Vortex Lattice (AVL) Software from the Massachusetts Institute of Technology (MIT) [16]. The AVL software is normally applied to aerodynamic and flight dynamic analysis of rigid aircraft, with arbitrary configurations. The modal properties of the EOLO structure, obtained from the Ground Vibration Test (GVT) by [26], is summarized in Table2.

Table 2 – Modal properties of the EOLO aircraft.

Mode	f (Hz)	Damping, ζ (%)
1st symmetric wing bending	4.6	1.6
Tail-boom torsion	7.7	2.1
1st asymmetric wing bending + tail-boom torsion	10.6	2.2
1st asymmetric wing bending + tail-boom torsion	11.6	1.2
1st symmetric wing torsion + tail-boom bending	15.0	1.7
1st asymmetric wing torsion	19.1	3.2
2nd symmetric wing bending + symmetric wing torsion	21.2	3.8
2nd asymmetric wing bending	30.4	2.4

On the other hand, the longitudinal elastic derivatives presented in [26] for EOLO wing were obtained using Waszak formulation, which is based on the modal shapes obtained from a Ground Vibration Test (GVT) [21]. All these parameters were applied to generate synthetic data, used to perform preliminary tests with subspace algorithms, and comparing with results obtained from the identification using experimental data.

3.2 Open-loop Subspace Identification

Among the four sequences of the flight test, the third one was performed in open-loop operation and had a total time of about 24 min. Maneuver sequences were executed to perform the system identification and a part of the time histories were split into seven-time windows as shown in Figure

3. The time histories depicted are related to the control surfaces deflections, aileron (right and left), rudder and elevator, and the throttle position (or throttle command).

In flight, about a straight and level flight condition, and varying the velocity from 10 m/s to 23 m/s, approximately, it was observed by the human pilot, that the EOLO aircraft began to vibrate uncontrollably at velocities of about 20 m/s. Then, flight tests using larger velocities were avoided. In time histories presented in Figure 3, there were maneuvers set of 3-2-1-1 and doublet signal applied to the elevator input. The sampling rate of the data acquisition was 100 Hz.

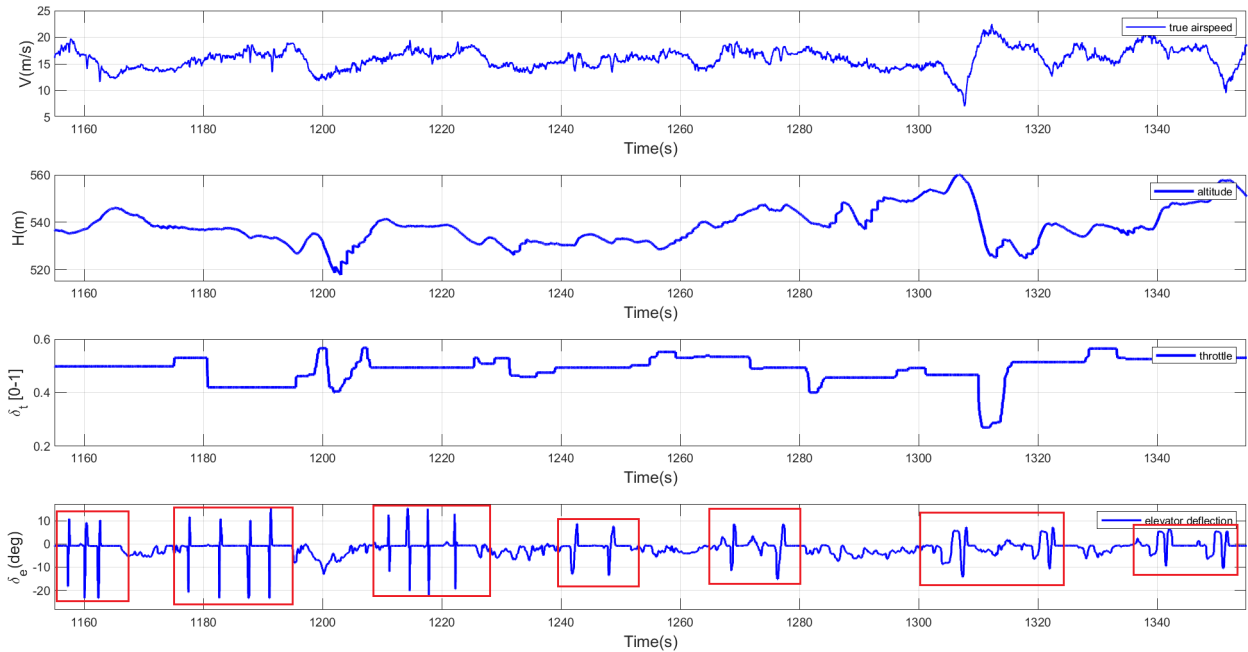


Figure 3 – Time histories of the open-loop aircraft: (a) true airspeed V , (b) altitude H , (c) throttle position δ_t , and (d) elevator deflection δ_e , for time window from 1155 s to 1355 s.

In order to check the capability of the elevator deflection to excite the dynamic system, the energy spectra plots of the elevator maneuvers for each data set are depicted and analyzed. According to plots in Figure 4, the 3-2-1-1 maneuver, applied in time intervals from 1300 s to 1325 s, exhibited a richer spectrum. Since the objective was to identify the aircraft longitudinal dynamics, this data set was used during the subspace algorithm application, according to results presented in this section. In general, the 3-2-1-1 maneuver has frequency components below 10 rad/s.

It is important to remark that the Indicated AirSpeed (IAS) was provided by the data acquisition system. Keeping the low speed, where the air compressibility is negligible (constant air density), the indicated airspeed is close to True AirSpeed (TAS), also named V . Therefore, for the results discussed in this section, involving experimental data, the indicated airspeed is equal to true airspeed, under this assumption.

In order to apply the DSR_e algorithm, the time histories for time window from 1300s to 1325 were split in an identification set with $N_{ident} = 1251$ and a validation data set $N_{val} = 1250$. The Matlab function `detrend` was applied to remove all bias and trends from the open-loop experimental data.

From time histories of the accelerometers, it was plotted the energy spectra of these signals in order to verify the most significant accelerometers' responses from the point of view of frequency contents. In this sense, the energy spectra from output responses of the five accelerometers are depicted in Figure 5. As a first identification procedure, these accelerometers data were used to perform the open-loop system identification, but were not observed improvements in the identification results obtained. This was the reason for the open-loop subspace identification have been applied to only the output responses of pitch rate q , true airspeed V , and pitch angle θ .

The open-loop subspace identification was performed using experimental EOLO input-output data. The measured inputs were the elevator deflections and the throttle positions. The pitch rate q , the

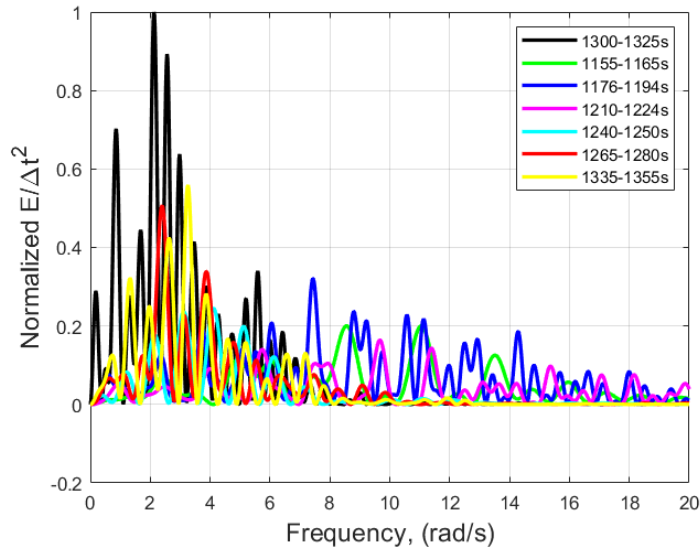


Figure 4 – Comparison of the energy spectra of the elevator deflections for the seven data set.

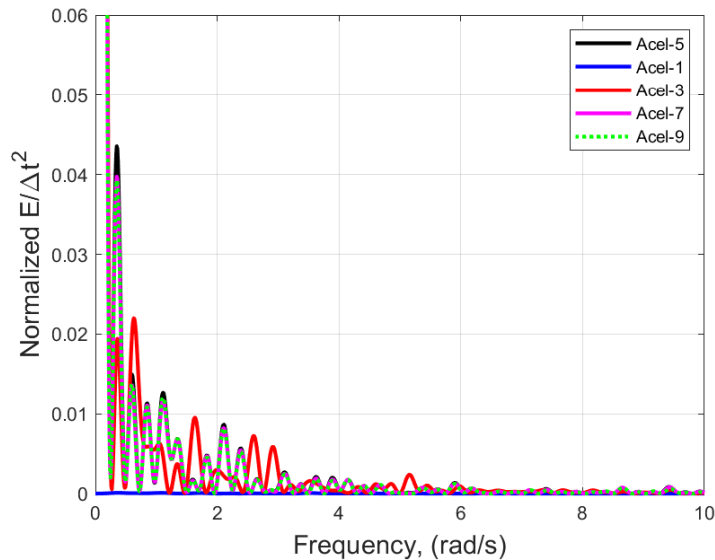


Figure 5 – (a) Comparison between the energy spectra of the accelerometers data related to Acel-1, Acel-3, Acel-5, Acel-7 and Acel-9.

true airspeed V , and the pitch angle θ , with exception of the altitude H , were used in the subspace algorithm. As the accelerometer data of the IMU (Inertial Measurement Unit) have not also improved the identification results, they were not used to identify the linear longitudinal model. Therefore, two system inputs, and three measured outputs, were used for system identification.

After detrending the open-loop experimental data, the block Hankel matrices were built using a past horizon $J = 200$ and a future horizon $L = 4$. Applying the DSR_e algorithm, a SVD decomposition was performed and a model order estimate $n = 4$ was obtained, based on the most significant singular values from the plot in Figure 6.

Although the identified model does not present the stability and control derivatives, the estimated discrete matrices obtained from the DSR_e algorithm performed are a similarity transformation of the

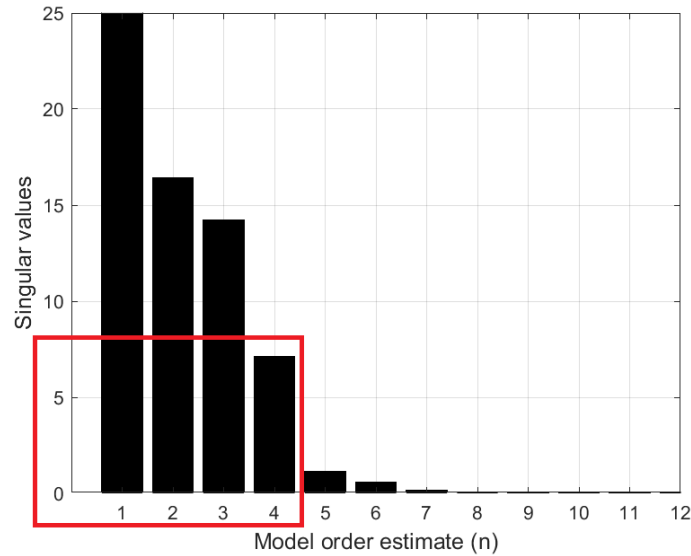


Figure 6 – Model order estimate based on the SVD decomposition, for identification parameters, past horizon $J = 200$ and future horizon $L = 4$.

real system. Thus, the discrete time linear model identified in open-loop is:

$$\begin{aligned}
 \mathbf{A} &= \begin{bmatrix} 1.0004 & 0.0196 & -0.0007 & -0.0476 \\ -0.0009 & 0.9975 & -0.0090 & 0.0203 \\ 0.0002 & -0.0119 & 0.9602 & -0.0061 \\ -0.0088 & 0.0565 & 0.3882 & -0.4514 \end{bmatrix} \\
 \mathbf{B} &= \begin{bmatrix} -0.0110 \\ -0.0250 \\ -0.0590 \\ 0.5828 \end{bmatrix} \\
 \mathbf{C} &= \begin{bmatrix} -0.2367 & 0.7813 & 2.1534 & 0.0551 \\ -9.7155 & 0.1266 & -0.2521 & 0.1903 \\ 0.3800 & 2.2511 & -0.7313 & 0.0257 \end{bmatrix} \\
 \mathbf{D} &= \begin{bmatrix} -0.0282 \\ -0.6955 \\ -0.0074 \end{bmatrix} \\
 \mathbf{K} &= \begin{bmatrix} 18.9035 & 1.3392 & 0.8768 \\ -2.9461 & -0.1493 & -2.6047 \\ 1.2696 & 0.1068 & -2.6047 \\ 2.1353 & -0.2380 & 44.1748 \end{bmatrix}
 \end{aligned}$$

where $z_{1,2} = 1.0001 \pm j0.0047$, $z_3 = -0.1354$ and $z_4 = 0.9567$ are the eigenvalues of dynamic matrix \mathbf{A} . Up to this point, it is important to remark that the system identification was performed only with three longitudinal motion variables, since an air data boom, for measurement of the aerodynamic angles, α and β , was not already installed.

According to preliminary results involving the previous flight envelope for the EOLO, based on synthetic data from the nonlinear model, it can be observed that the reference flight conditions are most affected (especially the angle of attack) by the true airspeed, and for this case, different altitudes practically does not vary the flight envelope. Therefore, the model predicted outputs for the identification displayed in Figure 7 may be improved, if information of the angle of attack α is added. Further, the goal will be to obtain the system identification also using measurements of the angle of attack and sideslip angle and later to evaluate the results obtained.

Now, it is known from Flight Mechanics that, for the longitudinal dynamic equations, more specifically,

for the ones used on short period approximation, some information about the variables α and q are needed to describe this mode. This is similar to the phugoid approximation, where the variables V and θ are also needed.

Although the algorithm has been applied in the absence of the aerodynamic angle α , the obtained results are still suitable since this is not a limitation of the identification algorithm, but a problem in generating richer input-output data, beyond the need for more identification variables associated to the flexible modes that want to identify.

After discussing some difficulties encountered in this work, and in order to provide informative data for system identification of the EOLO, it is important to remark that, based on experimental modal analysis, modal information may be obtained from both strain-gauges and accelerometers sensors [28].

One way consists in estimate the modal shapes, frequencies and generalized mass, and from the displacement estimates, it is possible to determine the modal coordinates, which may be used for system identification. This explanation is linked to concepts of elastic deformation on the flight dynamics of the vehicle, well described in [20] and also applied by [22].

Therefore, an important aspect is that in practical application it is necessary to add to the rigid-body variables the flexible effect information, just to improve the identified model for the same frequency range of interest desired. In this work, information from accelerometers sensors, attached along the wing structure installed to collected flight data, were used to perform the open-loop system identification. However, as already mentioned, they did not improve the identified model and, therefore, they were not used for modeling.

Another way to present the identification results is by exhibiting the Bode plots, as shown in Figure 8. This is actually more interesting from the point of view of dynamic analysis and control system design. In this case, the Bode magnitude and phase plots related to elevator deflections are exhibited (in black), and were provided from the linearized equations of motion, about the reference "trim" condition of straight and level flight, for velocities of 13 m/s, 16 m/s, 19 m/s, 22 m/s and 25 m/s at, and a fixed altitude of 547 m.

The Bode plots from the experimental open-loop data are exhibited (in blue) in Figure 8. Note that, as expected, due to the narrow energy spectra of the elevator 3-2-1-1 maneuver, the frequency components excited were limited to values below 10 rad/s. From the results obtained, it was observed that there was a similar behavior between the linearized model of the equations of motion and the identified model from experimental data. This seems reasonable since, from the GVT tests [29], it was not possible to observe the influence of the flexible modes in the low-frequency rigid-body dynamics. This similarity in both results seems an indication that the preliminary aerodynamic coefficients are valuable initial estimates for modeling the EOLO aircraft and a more accurate model needs to be reached.

A model validation criteria, for the open-loop subspace identification in time domain performed in this paper to evaluate the quality of the identified model, is the Mean Relative Squared Error (MRSE), which is defined as [15]:

$$MRSE(\%) = \frac{1}{l} \sum_{q=1}^l \left[\sqrt{\frac{\sum_{k=1}^{val} (y_{k,q} - \hat{y}_{k,q})^2}{\sum_{k=1}^{val} y_{k,q}^2}} \right] \times 100 \quad (4)$$

where $y_{k,q}$ is the q -th measured output, $\hat{y}_{k,q}$ is the q -th estimated output by the model, l is the output number of the system and val is the number of samples used for validation. A MRSE value equal to zero indicates a perfect fit.

A comparison of the identified model performance, as a function of the model order n , is summarized in Table3. The MRSE was calculated for both the identification and the validation data set. The model predicted outputs in Figure 7 exhibited unstable behavior, similar to the previous results obtained from the simulated model, and the variables with the larger MRSE are the true airspeed V and angle of attack θ , both associated to the phugoid mode.

4. Remarks on the system identification

In the previous section, it was presented the system identification without measurements of the angle of attack and sideslip angle and the results showed a model with a certain representative. In this

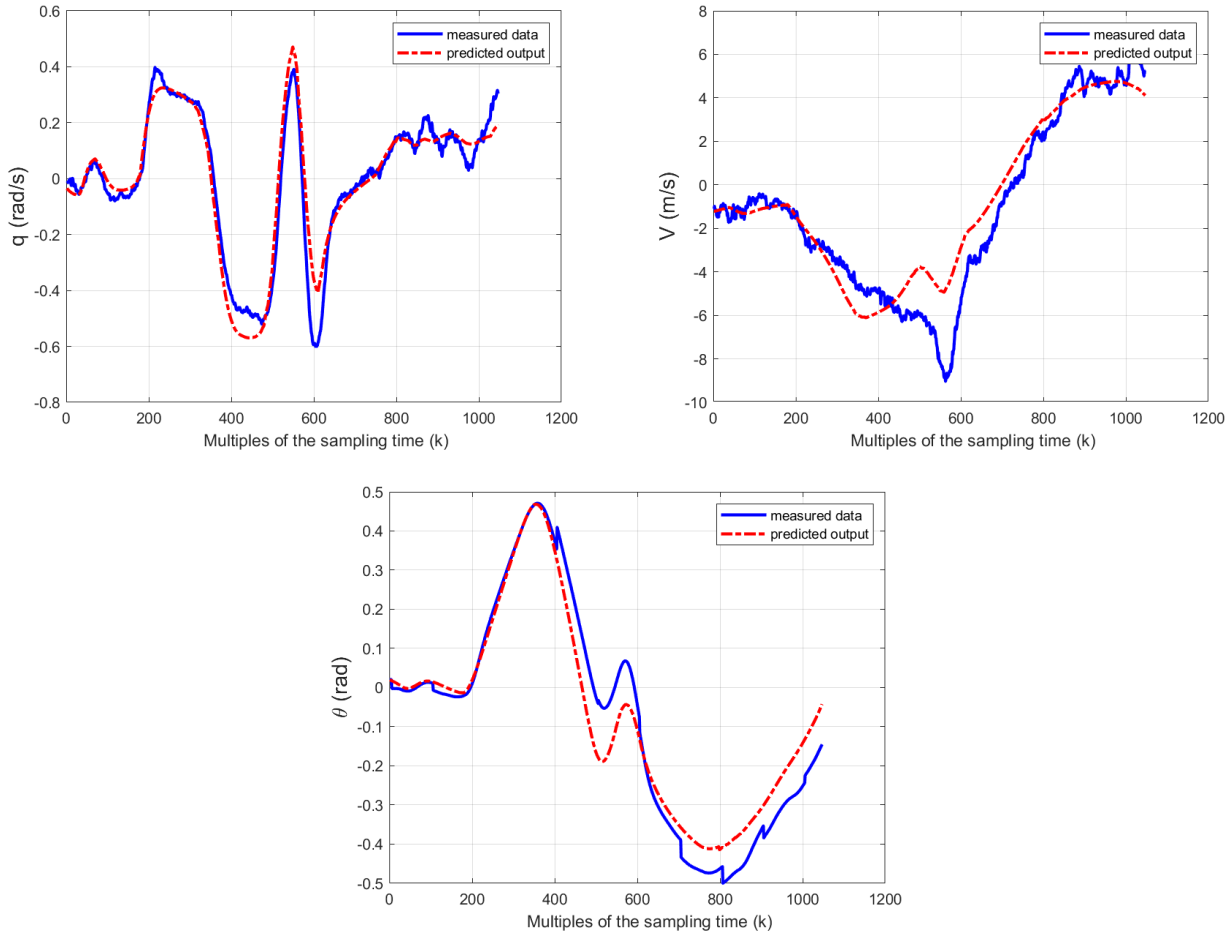


Figure 7 – Model predicted outputs related to q , V and θ variables for the identification data set.

section, the goal is to compare the system identification with and without these measurements. A simulated model of Rockwell-B1 aircraft was used to generate the identification data.

The mathematical model used to develop the simulation is available in the open literature [19] and a source-code, implemented by the author, is in Matlab/Simulink®. Additionally, some results about the subspace identification of Rockwell-B1 aircraft were presented in [3].

The same identification procedure presented in the previous section was applied to simulated data of Rockwell-B1 aircraft. To compare the system identification, it was assumed a fourth-order model for the aircraft longitudinal dynamics and the model predicted outputs were obtained for both cases, with and without measurements of the angle of attack. The model predicted outputs are shown in Figure 9 and Figure 10.

In order to compare the model representative, the MRSE validation criteria was calculated and the Table 4 presented the obtained results. It is possible to notice better predicted outputs when the angle of attack is used for system identification. Also, from analysis and as expected, it was observed that the worst predictions are related to short period mode.

5. Conclusions

This paper presented an open-loop identification procedure using the subspace methods for flight vehicle system identification of an Unmanned Aerial System (UAS) with rigid-body dynamic coupled with flexible dynamic. The results from experimental data of the aircraft operating in open-loop suggest good identification results. Therefore, this approach can be applied to the aircraft system identification with suitable performance.

According to results, a model with a certain representative even in absence of the angle of attack was identified within the frequency range of the system input. From collected data, it was not possible to identify the flexible dynamic, due to the excitation signal not having enough energy in that frequency

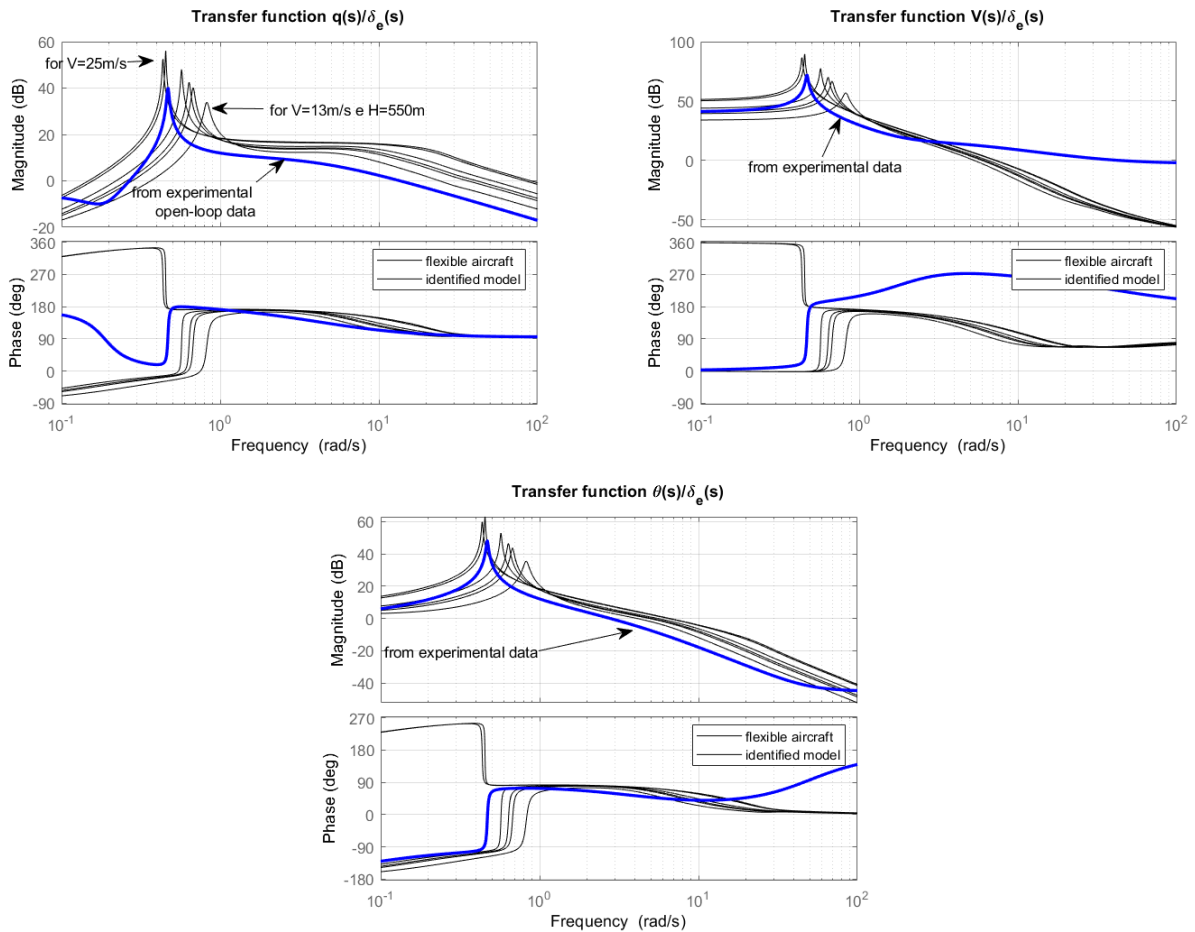


Figure 8 – Bode plots of the ratio of output variables q , V , θ to elevator deflection δ_e of the identified model from open-loop data.

band. Furthermore, it is expected that the identification results of the EOLO aircraft will be improved by addition of measurements of angle of attack and sideslip angle.

Although the partial derivatives related to the motion variables and control inputs do not appear explicitly in the model, there are modern control system designs that are based only on state-space models. Thus, the subspace approaches are an alternative to identify a representative model for the aircraft in open-loop operation. Moreover, SIM methods do not suffer the inconveniences encountered in applying classical methods.

6. Copyright Statement

The authors confirm that they, and/or their company or organization, hold copyright on all of the original material included in this paper. The authors also confirm that they have obtained permission, from the copyright holder of any third party material included in this paper, to publish it as part of their paper. The authors confirm that they give permission, or have obtained permission from the copyright holder of this paper, for the publication and distribution of this paper as part of the ICAS proceedings or as individual off-prints from the proceedings.

OPEN-LOOP SUBSPACE IDENTIFICATION OF A FLEXIBLE UNMANNED AERIAL SYSTEM

Table 3 – MRSE values for open-loop system identification using the DSR_e algorithm for two different model orders. For identification parameters, past horizon $J=200$ and future horizon $L=4$.

model order	n=4		n=5	
data set	id. set	val. set	id. set	val. set
$MRSE_q$	27.35 %	63.82 %	27.53 %	63.33 %
$MRSE_V$	31.06 %	100 %	31.08 %	100 %
$MRSE_\theta$	23.95 %	100 %	23.87%	100 %
$MRSE_{\bar{y}}$	27.46 %	87.94 %	27.50 %	87.77 %

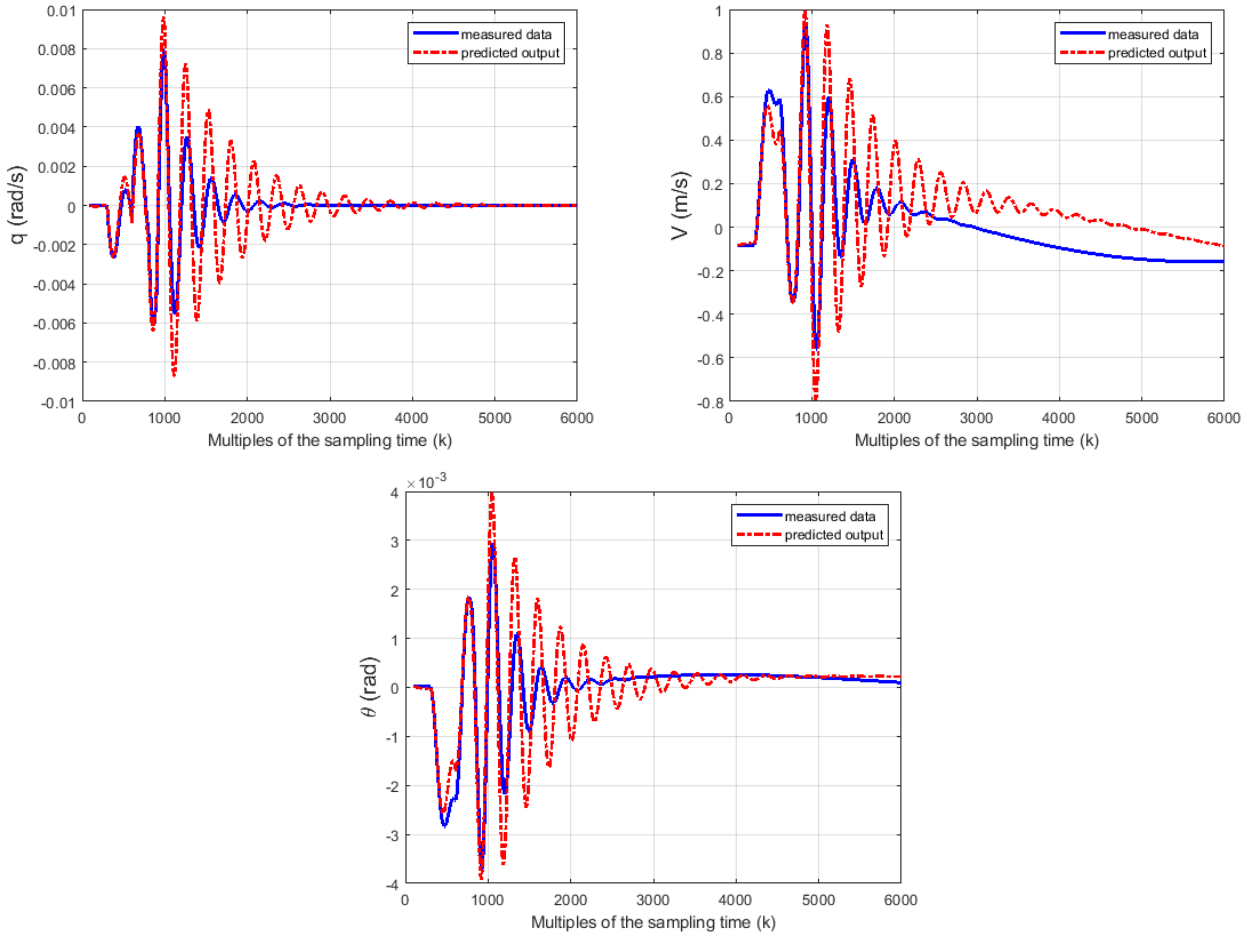


Figure 9 – Model predicted outputs related to q , V and θ variables for the identification data set without the measurements of the angle of attack.

Table 4 – MRSE values for open-loop system identification using the DSR_e algorithm without (first column) and with (second column) measurements of the angle of attack. For identification parameters, past horizon $J=90$ and future horizon $L=3$.

model order	n=4	n=4
data set	id. set	id. set
$MRSE_q$	80.28 %	1.01 %
$MRSE_V$	74.11 %	11.62 %
$MRSE_\alpha$	-	0.96 %
$MRSE_\theta$	63.67 %	5.38 %
$MRSE_{\bar{y}}$	72.69 %	4.74 %

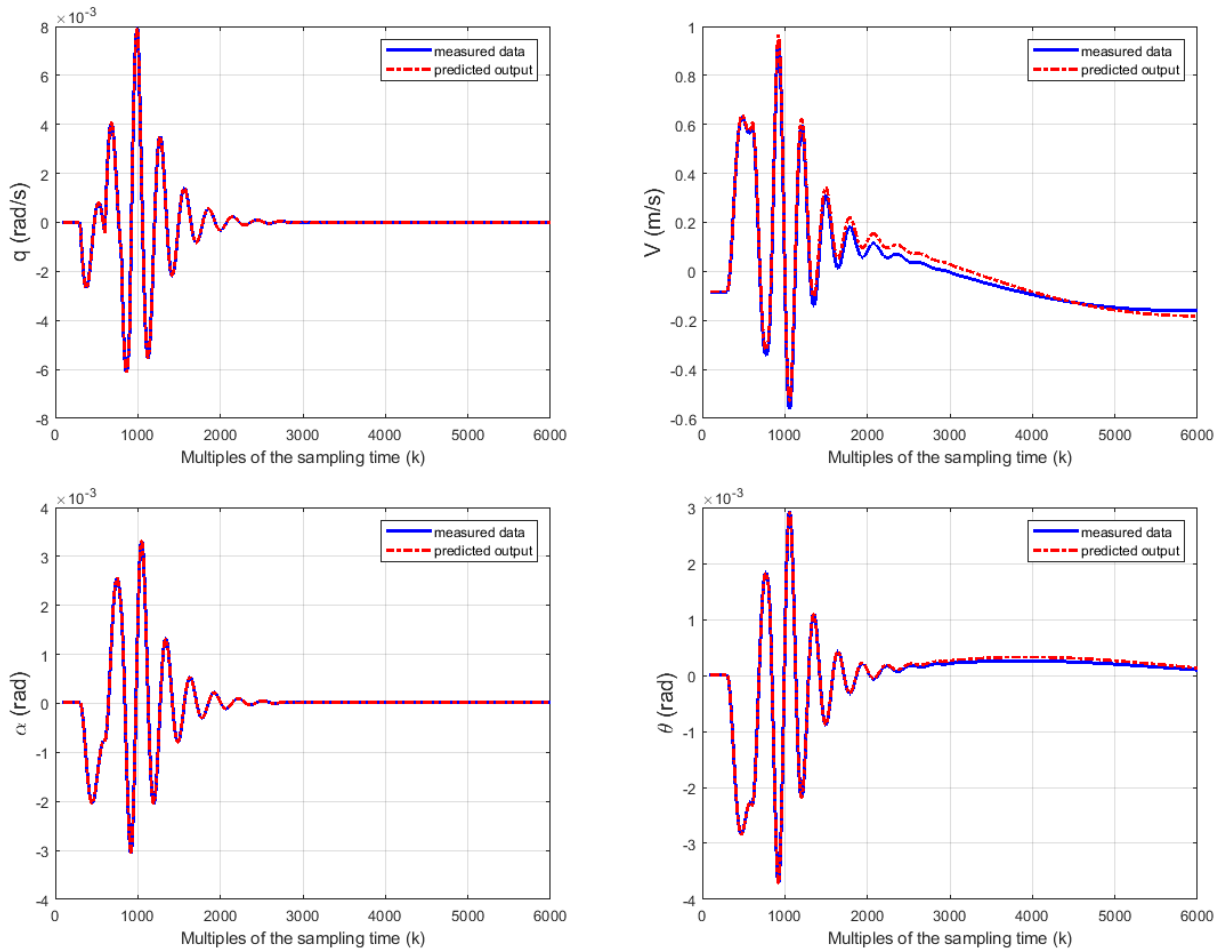


Figure 10 – Model predicted outputs related to q , V , α and θ variables for the identification data set.

References

- [1] ARMY Technology. Horus FT-100 Unmanned Aerial Vehicle (UAV). 2019. Accessed on 20 Oct. 2019. Available in: <<https://www.army-technology.com/projects/horus-ft-100-unmanned-aerial-vehicle-uav/>>.
- [2] Barbosa, G. et al. Design and flight test of a stability augmentation system for a flexible aircraft, *Proc of AIAA Scitech Forum*, California: AIAA, 2019.
- [3] Barbosa, R. C. M. G. and Góes, Luiz Carlos Sandoval. Closed-loop system identification of a large flexible aircraft using subspace methods, *Proc of 31st Congress of the International Council of the Aeronautical Sciences (ICAS)*, 2018.
- [4] Barbosa, R. C. M. G. *Closed-loop subspace identification of an Unmanned Aerial System (UAS) with flexible wings*. Thesis of Doctor of Science, Instituto Tecnológico de Aeronáutica (ITA), 2019.
- [5] Zúñiga D F C. *Aerolastic testing of flexible aircraft using acceleration and strain sensors*. Thesis of Doctor of Science, Instituto Tecnológico de Aeronáutica (ITA), 2019.
- [6] Di Ruscio D. Closed and open loop subspace system identification of the Kalman filter, *Modeling, Identification and Control*, pp 71-86, 2009.
- [7] Di Ruscio D. Combined deterministic and stochastic system identification and realization: DSR - a subspace approach based on observations, *Proc of Intl. Multi-Conf. on Engineering and Technological Innovation*, 2008.
- [8] Di Ruscio D. Combined deterministic and stochastic system identification and realization: DSR - a subspace approach based on observations, *Norwegian Society of Automatic Control*, pp 193-230, 1996.
- [9] Ferreira C O et al. Telemetria e sistema de aquisição de dados em voo para uma Aeronave Remotamente Pilotada (RPA), *TAS Journal*, pp 42-49, 2019.
- [10] Fischer C. *Identificação do modelo látero-direcional de um veículo aéreo não tripulado, VECTOR-P*. 99 p., Thesis of Master of Science - Instituto Tecnológico de Aeronáutica (ITA), 2017.
- [11] Jansson M. Subspace identification and ARX modeling, *IFAC Proceedings Volumes*, Vol. 36, No. 16, pp

1585-1590, 2003.

- [12] Katayama T. *Subspace methods for system identification*. Kyoto: Springer, 2005.
- [13] Overschee P V and De Moor B L R. *Subspace identification for linear systems: theory, implementations, applications*. Leuven: Kluwer Academic Publishers, 1996.
- [14] Maciel B C O. *Modelagem e identificação de aeronaves via abordagem de sistemas lineares com parâmetros variantes*. 173 p., Thesis of Doctor of Science - Instituto Tecnológico de Aeronáutica (ITA), 2008.
- [15] Machado R C. *Métodos de subespaços para identificação de sistemas em mlha fechada*. 144 p., Thesis of Master of Science - Instituto Tecnológico de Aeronáutica (ITA), 2013.
- [16] MIT. AVL Software, Accessed on 20 Oct. 2019. Available in: <<http://web.mit.edu/drela/Public/web/avl/>>.
- [17] Ramirez P J G. *Loop-separation control for very flexible aircraft*. 188 p., Thesis of Doctor of Science, Instituto Tecnológico de Aeronáutica (ITA), 2019.
- [18] Santos S S. *Identificação e controle de um veículo aéreo não tripulado: Vector-P*, 123 p., Thesis of Master of Science - Instituto Tecnológico de Aeronáutica (ITA), 2013.
- [19] Schmidt D K. A non-linear simulink simulation of a large, flexible aircraft-FLEXSIM, Project supported by MUSYN, 2013.
- [20] Schmidt D K. *Modern flight dynamics*. New York: Mc Graw-Hill, 2012.
- [21] Schmidt D K and Waszak M. Flight dynamics of aeroelastic vehicles, *Journal of Aircraft*, Vol. 27, No. 6, pp 563-571, 1988.
- [22] Silva B G O and Mönnich W. System identification of flexible aircraft in time domain, *Proc of AIAA Atmospheric Flight Mechanics Conference*, Minneapolis: AIAA, 2012.
- [23] Voracek D. Research, technology, and engineering accomplishments. 2014. Accessed on 20 Oct. 2019. Available in: <<https://ntrs.nasa.gov/archive/nasa/casi.ntrs.nasa.gov/20140010467.pdf>>.
- [24] Souza A G, Zúñiga D F C, Góes L C S. Parameter identification for a flexible unmanned aerial vehicle using extended Kalman filtering, *Proc of XVIII International Symposium on Dynamic Problem of Mechanics*, 2019.
- [25] Souza A G, Góes L C S, Sousa M, Zúñiga D F C and Barbosa R C M G. Identificação de parâmetro da dinâmica longitudinal de uma aeronave flexível usando o método de erro na saída, *Proc of X Congresso Nacional de Engenharia Mecânica*, 2018.
- [26] Zúñiga D F C, Souza A G, Rios A and Góes L C S. Flight dynamics modeling of a flexible wing unmanned aerial vehicle, *Mechanical Systems and Signal Processing*, Vol. 145, 2020.
- [27] Zúñiga D F C, Souza A G and Góes L C S. Operational modal analysis using impulsive input of a flexible wing unmanned aerial vehicle. *Proc of XV International Symposium on Dynamic Problems of Mechanics*, 2019.
- [28] Zúñiga D F C, Souza A G and Góes L C S. Development of an aeroelastic in-flight testing system for a flexible wing unmanned aerial vehicle using acceleration and strain sensors, *Proc of AIAA Scitech Forum*, 2019.
- [29] Zúñiga D F C, Souza A G, Rios A and Góes L C S. Flight dynamics modeling of a flexible wing unmanned aerial vehicle, *Proc of International Conference on Structural Engineering Dynamics*, 2019.
- [30] Zúñiga, D F C, Souza A G and Góes L C S. Planning of an in-flight aeroelastic testing of a flexible unmanned aerial vehicle using a combined accelerometers-strain sensors operational modal analysis, *Proc of International Conference on Structural Engineering Dynamics*, 2019.